

# Journal of Intelligent Material Systems and Structures

<http://jim.sagepub.com/>

---

## **On the Effectiveness of Vibration-based Energy Harvesting**

Shad Roundy

*Journal of Intelligent Material Systems and Structures* 2005 16: 809

DOI: 10.1177/1045389X05054042

The online version of this article can be found at:

<http://jim.sagepub.com/content/16/10/809>

---

Published by:



<http://www.sagepublications.com>

**Additional services and information for *Journal of Intelligent Material Systems and Structures* can be found at:**

**Email Alerts:** <http://jim.sagepub.com/cgi/alerts>

**Subscriptions:** <http://jim.sagepub.com/subscriptions>

**Reprints:** <http://www.sagepub.com/journalsReprints.nav>

**Permissions:** <http://www.sagepub.com/journalsPermissions.nav>

**Citations:** <http://jim.sagepub.com/content/16/10/809.refs.html>

>> [Version of Record](#) - Sep 29, 2005

[What is This?](#)

# On the Effectiveness of Vibration-based Energy Harvesting

SHAD ROUNDY\*

*LV Sensors, 1480 64th St., Suite 175, Emeryville, CA 94608, USA*

**ABSTRACT:** There has been a significant increase in the research on vibration-based energy harvesting in recent years. Most research is focused on a particular technology, and it is often difficult to compare widely differing designs and approaches to vibration-based energy harvesting. The aim of this study is to provide a general theory that can be used to compare different approaches and designs for vibration-based generators. Estimates of maximum theoretical power density based on a range of commonly occurring vibrations, measured by the author, are presented. Estimates range from 0.5 to 100 mW/cm<sup>3</sup> for vibrations in the range of 1–10 m/s<sup>2</sup> at 50–350 Hz. The theory indicates that, in addition to the parameters of the input vibrations, power output depends on the system coupling coefficient, the quality factor of the device, the mass density of the generator, and the degree to which the electrical load maximizes power transmission. An expression for effectiveness that incorporates all of these factors is developed. The general theory is applied to electromagnetic, piezoelectric, magnetostrictive, and electrostatic transducer technologies. Finally, predictions from the general theory are compared to experimental results from two piezoelectric vibration generator designs.

*Key Words:* vibrations, energy scavenging, energy harvesting, efficiency, effectiveness.

## INTRODUCTION

THE rapidly decreasing size, cost, and power consumption of sensors and electronics has opened up the relatively new research field of energy harvesting. The goal, of course, is to harvest enough ambient energy to power a standalone sensor and/or actuator system. A lot of research has been done in recent years on using ambient vibrations as a power source. Most of this research has been focused on technology-specific solutions. For example, Amirtharajah and Chandrakasan (1998), El-hami et al. (2001), and Ching et al. (2002) have developed electromagnetic generators. Meninger et al. (2001), Miyazaki et al. (2003), Roundy et al. (2002), and Sterken et al. (2003) have worked on electrostatic generators. Ottman et al. (2003), Glynne-Jones et al. (2001), and Roundy et al. (2004) have developed piezoelectric vibration-based generators. All three of these basic methods of generating power from vibrations have been successfully demonstrated. Additionally, some of these generators have successfully powered wireless transceivers (Ottman et al., 2003; Roundy et al., 2003).

While there have been many publications that document successfully developed generators, a solid basis for comparison between basic technologies has not

been published, to the author's knowledge. It is, therefore, appropriate to step back and ask what is the maximum amount of power available from real-world vibration sources, and what is a good basis to compare the effectiveness of different vibration-to-electricity conversion methods? The aim of this study, then, is to present such a basis for comparison and a basis for very quickly determining how much power could be generated from a given vibration source.

A basic, technology independent, theory is presented first. The theory is then applied to electromagnetic, piezoelectric, magnetostrictive, and electrostatic transducer technologies. The results of measurements on a wide range of commonly occurring vibrations are then presented, and the basic theory is applied to those vibration sources. Finally, the general theory is compared to the experimental results for two piezoelectric generators.

## BASIC THEORY

The efficiency of a given design is often requested, and sometimes supplied, while discussing a particular vibration-based generator. However, in the context of vibration-based energy harvesting, the concept of efficiency is usually not very well defined. Sometimes efficiency is defined by summing up the losses due to factors like resistance of the coil, internal resistance

\*E-mail: sroundy@lvsensors.com

of the piezoelectric material, etc. It can also be defined by summing the losses in the power conversion circuitry. However, neither of these definitions reveals how much of the potential power supplied by the vibrations actually gets converted to electricity. The standard definition of efficiency is  $\eta = P_{\text{out}}/P_{\text{in}}$ , where  $P_{\text{out}}$  is the power delivered to the electrical load, and  $P_{\text{in}}$  is the power supplied by the vibrations. An equivalent definition of efficiency is  $\eta = U_{\text{out}}/U_{\text{in}}$ , where  $U$  is energy per cycle instead of power. Efficiency in this context is mathematically identical to what is sometimes referred to as the transmission coefficient ( $\lambda$ ) of a transducer (Wang et al., 1999). The definition of the commonly used coupling coefficient ( $k$ ) is sometimes worded in different ways depending on the specific application under consideration (Wang et al., 1999; Bright, 2001; Yaralioglu et al., 2003). However, the concept is always the same, both conceptually and mathematically. The coupling coefficient relates the total energy put into a system to the amount of energy that is converted by the transducer. If there is no load on the output of the transducer (such as a resistor or externally imposed mechanical force), then the square of the coupling coefficient is simply the energy stored at the output port divided by the total energy put into the system, which is equal to the total energy stored in the system if there is no external load. Mathematically, the coupling coefficient can be written as  $k^2 = U_{\text{st}}/U_{\text{in}}$ , where  $U_{\text{st}}$  is the energy stored at the output port when there is no external load and  $U_{\text{in}}$  is the total input energy, and is the same value used in the definition of transmission coefficient. While the coupling coefficient is related to efficiency and the transmission coefficient, they are not one and the same.

Using general equations for a linear transducer, the coupling coefficient ( $k$ ), transmission coefficient ( $\lambda$ ), and maximum output power ( $P_{\text{max}}$ ) are derived. Assume a standard two-port transducer as shown in Figure 1.

Assuming that the transducer is linear, the constitutive equations are given in Equation (1).

$$\begin{bmatrix} A_1 \\ A_2 \end{bmatrix} = \begin{bmatrix} q_{11} & q_{12} \\ q_{21} & q_{22} \end{bmatrix} \begin{bmatrix} T_1 \\ T_2 \end{bmatrix} \quad (1)$$

where  $A_1$  and  $A_2$  are the across variables,  $T_1$  and  $T_2$  are the through variables, and  $q_{ij}$  are proportionality constants. The names ‘across’ and ‘through’ for the variables indicate the states acting ‘across’ and ‘through’

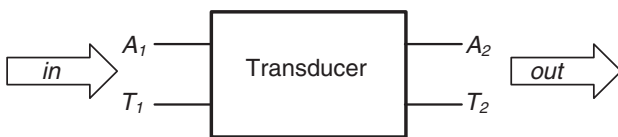


**Figure 1.** Standard two-port model of a transducer.  $A_1$  and  $T_1$  are the input across and through variables, respectively.  $A_2$  and  $T_2$  are the output variables (Bright, 2001).

an element. For example, the across variable for an electrical element is voltage (or flux linkage) and the through variable is current (or charge). The across variable for a spring is velocity (the velocity must be measured on either side, thus velocity is acting ‘across’ the spring) and the through variable is force. Multiplying the across and through variables at an instant in time results in the power (or energy) of the element. In contrast to simple elements, a transducer has two sets of across and through variables representing the states in each of its two domains. For example, the across and through variables at the mechanical port of an electromagnetic transducer are velocity and force, respectively, and the across and through variables at the electrical port are voltage across the coil and current through the coil.

The coupling coefficient ( $k$ ) is defined as in Equation (2). As this term is well defined (Bright, 2001), it need not be derived here. However, note that it is only dependent on the proportionality constants and not on any load condition. This is because it is defined using the energy stored at the output port rather than energy transferred to a load.

$$k^2 = \frac{q_{12}^2}{q_{11}q_{22}} \quad (2)$$

To derive the transmission coefficient, the input and output energy terms need to be defined. We assume that energy is put into the system by changing the through variable at the input port while keeping the across variable constant. Then, the input energy is defined by Equation (3).

$$U_{\text{in}} = A_1 \int_0^{T_1} dT_1 \quad (3)$$

Substituting  $A_1 = q_{11}T_1 + q_{12}T_2$  into Equation (3) yields the expression in Equation (4).

$$U_{\text{in}} = \frac{1}{2}q_{11}T_1^2 + q_{12}T_1T_2 \quad (4)$$

In a similar manner, the output energy, or energy transferred to an external load, can be defined as shown in Equation (5).

$$U_{\text{out}} = \frac{1}{2}q_{22}T_2^2 + q_{21}T_1T_2 \quad (5)$$

The transmission coefficient is defined as  $\lambda = U_{\text{out}}/U_{\text{in}}$  and therefore is given by Equation (6).

$$\lambda = \frac{T_2(q_{21}T_1 + (1/2)q_{22}T_2)}{T_1((1/2)q_{11}T_1 + q_{12}T_2)} \quad (6)$$

If we substitute  $T_1$  and  $T_2$  with the ratio  $a = T_2/T_1$ , the resulting expression for the transmission coefficient is:

$$\lambda = \frac{(1/2)q_{22}a^2 + q_{21}a}{(1/2)q_{11} + q_{12}a} \quad (7)$$

Clearly, the transmission coefficient, unlike the coupling coefficient, is dependent on the load condition (expressed here as the ratio  $a$ ). If the output is constrained such that the through variable ( $T_2$ ) is zero, then  $\lambda=0$ . Likewise, if the output is constrained such that the across variable ( $A_2$ ) is zero, then  $T_2=-q_{21}/q_{22}T_1$ ,  $a=-q_{21}/q_{22}$ , and  $\lambda=0$  again. It should also be noted that the transmission coefficient is not necessarily constant in time. The load conditions may change. In particular, power circuits incorporating nonlinear electrical loading can improve power transmission (Ottman et al., 2003). However, regardless of whether the external load is linear or not, Equation (7) accurately describes the transmission coefficient as long as the underlying behavior of the transducer itself is linear.

We are interested in the transmission coefficient at which the output energy is maximum ( $\lambda_{max}$ ). Assuming linear transducer relationships, the potential values of the output variables ( $A_2$  and  $T_2$ ) are shown by the line in Figure 2.  $A_{2o}$  is the value of the across variable when  $T_2$  is constrained to be zero, and  $T_{2o}$  is the value of the through variable when  $A_2$  is constrained to be zero. Note that the procedure used here is similar to that used by Wang et al. (1999). The maximum output energy state ( $U_{max}$ ) occurs when  $A_2=A_{2o}/2$  and  $T_2=T_{2o}/2$ , as shown in Figure 3. Thus the maximum output energy is given by:

$$U_{max} = \frac{1}{4} A_{2o} T_{2o} \tag{8}$$

From Equation (1), if  $A_2=0$ , then  $T_{2o}$  is:

$$T_{2o} = -\frac{q_{21}}{q_{22}} T_1 \tag{9}$$

If  $T_2=T_{2o}/2$ , then  $A_2=A_{2o}/2$  (see Figure 2). Thus, referring to Equation (1):

$$\frac{1}{2} A_{2o} = q_{21} T_1 + \frac{1}{2} q_{22} T_{2o} \tag{10}$$

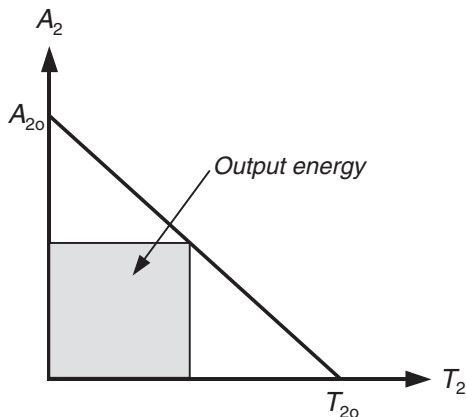


Figure 2. Relationship of the output variables  $T_2$  and  $A_2$ , showing the maximum energy state at  $A_2=A_{2o}/2$  and  $T_2=T_{2o}/2$ .

Substituting Equations (9) and (10) into Equation (8) yields the following expression for  $U_{max}$ :

$$U_{max} = -\frac{1}{4} \frac{q_{21}^2}{q_{22}} T_1^2 \tag{11}$$

The maximum output energy appears as a negative number because it represents energy leaving the system as opposed to that entering the system. In practice, we are only concerned about the magnitude of the output energy term, and so it will be treated as a positive value in deriving the maximum transmission coefficient.

Assuming that  $T_2=T_{2o}/2$ , and substituting Equation (9) into Equation (4) results in the following expression for input energy:

$$U_{in} = \left( q_{11} - \frac{q_{12}q_{21}}{2q_{22}} \right) T_1^2 \tag{12}$$

The maximum transmission coefficient is then  $\lambda_{max} = U_{max}/U_{in}$  and is given by Equation (13).

$$\lambda_{max} = \frac{q_{21}^2}{4q_{11}q_{22} - 2q_{12}q_{21}} \tag{13}$$

We now assume that  $q_{21}=q_{12}$ , which is generally the case for linear transducers. Substituting Equation (2) into Equation (13) and simplifying yields the following expression for  $\lambda_{max}$ :

$$\lambda_{max} = \frac{k^2}{4 - 2k^2} \tag{14}$$

Thus, the maximum transmission coefficient depends only on the coupling coefficient, but is not equivalent to it. Note also that the  $\lambda_{max}$  is independent of loading conditions. This is because it represents the theoretical maximum output to input ratio. Figure 3 shows the curve relating  $\lambda_{max}$  to the coupling coefficient ( $k$ ). As noted earlier, the actual transmission coefficient ( $\lambda$ ) is dependent on the load condition and can vary anywhere from zero to  $\lambda_{max}$ . Thus, the system needs to be designed such that the apparent load maximizes the average actual transmission coefficient as nearly as possible.

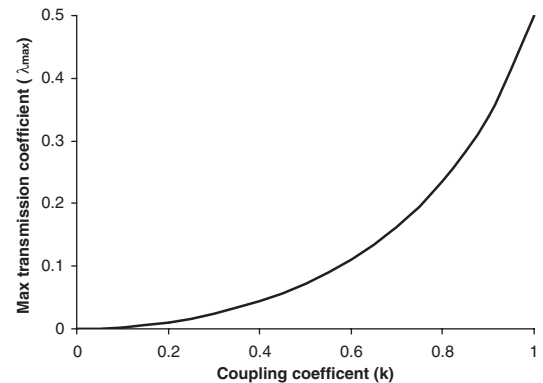


Figure 3. Maximum transmission coefficient ( $\lambda_{max}$ ) vs coupling coefficient ( $k$ ).

Finally, it is useful to develop a generic expression for maximum output power in terms of the parameters of the input vibrations and the system coupling coefficient. Naturally, the maximum output power is  $P_{\max} = dU_{\max}/dt$ . Assuming that the vibrational excitation, and thus the AC power signal is sinusoidal in nature, and recalling that  $U_{\max} = \lambda_{\max} U_{\text{in}}$ , the output power can be expressed as:

$$P_{\max} = \lambda_{\max} \omega U_{\text{in}} \quad (15)$$

where  $\omega$  is the circular frequency of driving vibrations,  $U_{\text{in}}$  is given by Equation (12), and  $\lambda_{\max}$  is given by Equation (14).

### BASIC THEORY APPLIED TO SPECIFIC TECHNOLOGIES

The basic theory already presented is applied to electromagnetic, piezoelectric, magnetostrictive, and electrostatic transducer technologies. In the application to specific technologies, a more specific general equation for power density will emerge.

#### Electromagnetic

The constitutive equations for a simple oscillating electromagnetic transducer are given by

$$\begin{bmatrix} F \\ \lambda' \end{bmatrix} = \begin{bmatrix} k_{\text{sp}} & Bl \\ Bl & L \end{bmatrix} \begin{bmatrix} z \\ i \end{bmatrix} \quad (16)$$

where  $F$  is force,  $\lambda'$  is the flux linkage,  $k_{\text{sp}}$  is the stiffness of a restoring spring,  $B$  is the magnetic field,  $l$  is the total length of the conductor (usually a coil),  $L$  is the inductance of the conductor,  $z$  is the relative displacement of the conductor and magnetic field, and  $i$  is the current in the conductor.

By direct substitution into Equation (2), the coupling coefficient is given by the following expression

$$k^2 = \frac{(Bl)^2}{k_{\text{sp}}L} \quad (17)$$

Direct substitution into Equation (11) yields

$$U_{\max} = \frac{(Bl)^2}{4L} z^2 \quad (18)$$

Noting the similarity between Equations (17) and (18),  $U_{\max}$  can be written as:

$$U_{\max} = \frac{k_{\text{sp}}k^2}{4} z^2 \quad (19)$$

Likewise, direct substitution into Equation (12) yields

$$U_{\text{in}} = \left( k_{\text{sp}} - \frac{(Bl)^2}{2L} \right) z^2 \quad (20)$$

Again noting the similarity between Equations (20) and (17),  $U_{\text{in}}$  can be written as:

$$U_{\text{in}} = \left( 1 - \frac{k^2}{2} \right) k_{\text{sp}} z^2 \quad (21)$$

The maximum transmission coefficient ( $\lambda_{\max}$ ) can be obtained by substituting Equation (17) into Equation (14). These substitutions will yield an expression for maximum power output in terms of the relative displacement ( $z$ ). However, a more useful expression would give the maximum output power in terms of the parameters of the input vibrations. Thus, a general relationship between the displacement ( $z$ ) and the parameters of the input vibrations needs to be found.

Most inertial vibration-based generator consists of an oscillating spring and mass system as shown in Figure 4 (Mitcheson et al., 2004). The input vibrations are represented as  $y(t)$ . The relative motion between magnetic field and conductor is represented by the relative motion between the housing and proof mass (or the spring deflection in Figure 4). Assuming that this is a resonant system, the spring deflection ( $z(t)$ ) can be expressed as  $z(t) = Qy(t)$  where  $Q$  is the quality factor, given as  $Q = 1/(2\zeta)$ .  $\zeta$  is the dimensionless damping ratio and is related to the damping constant ( $b$ ) shown in Figure 4 by  $b = 2m\zeta\omega_n$ , where  $\omega_n$  is the system natural frequency.

The AC magnitude of the spring deflection is then  $|Z| = Q|Y|$ . However, it is more common to refer to vibrations in terms of acceleration magnitude rather than displacement magnitude. Recalling that  $|A| = \omega^2|Y|$  where  $|A|$  is the acceleration magnitude of the input vibrations (referred to as just  $A$  hereafter), we can write the magnitude of the spring deflection as

$$|Z| = \frac{QA}{\omega^2} \quad (22)$$

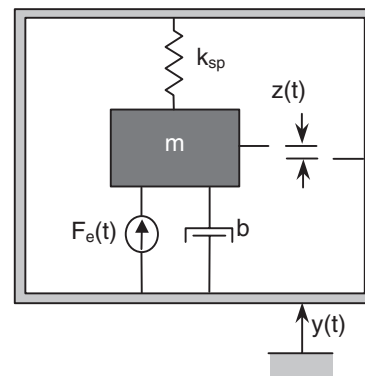


**Figure 4.** Schematic of basic, non-technology specific, vibration-based generator.  $F_e(t)$  is the force generated by the mechanical-electrical coupling,  $k_{\text{sp}}$  is the spring constant,  $b$  is the damping coefficient,  $y(t)$  is the displacement of the input vibrations, and  $z(t)$  is the spring deflection.

Substituting Equation (22) into Equation (21) yields

$$U_{in} = \left(1 - \frac{k^2}{2}\right) \frac{k_{sp}(QA)^2}{\omega^4} \quad (23)$$

Note that  $k_{sp} = m\omega_n^2$  where  $\omega_n$  is the natural frequency of the system. As mentioned before, we are assuming a resonant system. Therefore,  $\omega_n = \omega$ . Substituting into Equation (23) yields the final expression for  $U_{in}$ .

$$U_{in} = \left(1 - \frac{k^2}{2}\right) \frac{m(QA)^2}{\omega^2} \quad (24)$$

Substituting Equations (24) and (14) into Equation (15) and simplifying results in

$$P_{max} = \frac{k^2 m(QA)^2}{4\omega} \quad (25)$$

Normalizing for size, the expression for power density is

$$p_{max} = \frac{k^2 \rho(QA)^2}{4\omega} \quad (26)$$

where  $\rho$  is the density of the proof mass material, and  $p_{max}$  is power density in  $W/m^3$  or the equivalent  $\mu W/cm^3$ .

Note that the output power is dependent on the level of mechanical damping, which determines  $Q$ . However, the maximum transmission coefficient ( $\lambda$ ) does not depend on damping. The reason is that the input energy (or power) used in the derivation of  $\lambda$  only considers the energy at the input port of the transducer, which is the energy imparted by the oscillating proof mass, not the energy input by the vibrations. However, when  $U_{in}$  is defined as in Equation (24) the relationship between the displacement of the proof mass and the input accelerations is accounted for. The maximum transmission coefficient depends on the suitability of the technology or material chosen as a transducer while  $U_{in}$  depends primarily on the design of the overall oscillating system and the parameters of the input vibrations. As a result, effects of all three (material, design, and input vibrations) appear in the power expression.

### Piezoelectric Application

The constitutive equations for a piezoelectric material are given by

$$\begin{bmatrix} S \\ D \end{bmatrix} = \begin{bmatrix} s & d \\ d & \varepsilon \end{bmatrix} \begin{bmatrix} T \\ E \end{bmatrix} \quad (27)$$

where  $S$  is the strain,  $D$  is the electrical displacement,  $s$  is the compliance,  $d$  is the piezoelectric strain coefficient,  $\varepsilon$  is the dielectric constant,  $T$  is the stress, and  $E$  is the electric field.

By direct substitution into Equation (2), the coupling coefficient is given by the following familiar expression:

$$k^2 = \frac{d^2}{s\varepsilon} = \frac{d^2 Y}{\varepsilon} \quad (28)$$

where  $Y$  is the elastic constant or Young's modulus.

Again by direct substitution into Equations (11) and (12), the maximum output energy ( $u_{max}$ ) and the input energy ( $u_{in}$ ) are given by:

$$u_{max} = -\frac{1}{4} \frac{d^2}{\varepsilon} T^2 = -\frac{1}{4} \frac{k^2}{Y} T^2 \quad (29)$$

$$u_{in} = \left(\frac{1}{Y} - \frac{d^2}{2\varepsilon}\right) T^2 = \left(1 - \frac{k^2}{2}\right) \frac{T^2}{Y} \quad (30)$$

Note that the energy terms here are lower case  $u$  instead of upper case  $U$ . That is because the piezoelectric variables yield energy density rather than energy. The coupling coefficient and the transmission coefficient can just as easily be defined with energy density as with energy.

The maximum transmission coefficient ( $\lambda_{max}$ ) and maximum output power can be obtained by substituting Equations (28) and (30) into Equations (14) and (15). These substitutions will yield an expression for maximum power output in terms of the stress in the piezoelectric material ( $T$ ). We prefer an expression in terms of the input vibrations. Therefore, we will proceed to relate the stress to the input vibrations.

Referring back to Figure 4, we note that for most designs the piezoelectric material will constitute the restoring spring ( $k_{sp}$ ). The mass will exert some force ( $F$ ) on the piezoelectric material, given by  $F(t) = m\ddot{z}(t)$ . Therefore, the AC magnitude of this force can be written as  $|F| = mQA$ . Assuming a simple stack structure, the stress in the piezoelectric element is just  $T = |F|/a_p$  where  $a_p$  is the cross-sectional area of the piezoelectric stack. Then

$$u_{in} = \left(1 - \frac{k^2}{2}\right) \frac{(mQA)^2}{Ya_p^2} \quad (31)$$

The stiffness of that spring is  $k_{sp} = Ya_p/h$  where  $h$  is the height of the piezoelectric element. As before, we assume a resonant system such that  $k_{sp} = m\omega^2$ . Then we can write the following relationship:

$$\omega^2 = \frac{Ya_p}{hm} \quad (32)$$

Substituting Equation (32) into Equation (31) yields

$$u_{in} = \left(1 - \frac{k^2}{2}\right) \frac{(QA)^2 m}{\omega^2 h a_p} \quad (33)$$

The term  $h a_p$  is the volume of the piezoelectric material. Thus  $U_{in} = h a_p u_{in}$  and

$$U_{in} = \left(1 - \frac{k^2}{2}\right) \frac{(QA)^2 m}{\omega^2} \quad (34)$$

Finally, substituting Equations (34) and (14) into Equation (15) yields

$$P_{\max} = \frac{k^2 m (QA)^2}{4\omega} \quad (25)$$

And, normalizing for the size of the proof mass results in the following expression for power density:

$$p_{\max} = \frac{k^2 \rho (QA)^2}{4\omega} \quad (26)$$

As the equations for power and power density derived for the piezoelectric case are identical to those derived for the electromagnetic case, they have been numbered as Equations (25) and (26), referring back to the electromagnetic power equations. These two equations turn out to characterize the power and power density for any linear transducer technology.

The assumption of a simple piezoelectric stack at the geometric structure is somewhat unrealistic as the natural frequency would be far too high. A more likely scenario would be to use a bending element or a similar structure. However, in the case of other geometric structures, the input force can usually be related to the average stress in the piezoelectric material by some geometric constant ( $a_p$ ), the effective spring stiffness ( $k_{sp}$ ) can still be related to the elasticity of the material ( $Y$ ) by some other geometric constant ( $a_p/h$ ). Regardless of the structure, the units of  $h$  are length and the units of  $a_p$  are length squared. Therefore, the volume of the material is just then  $k'a_p h$  where  $k'$  is some constant. Then Equations (25) and (26) still apply for a piezoelectric material with a constant multiplicative factor ( $1/k'$ ).

### Magnetostrictive Application

Assuming small signal linear behavior, the constitutive equations for a magnetostrictive material are given by

$$\begin{bmatrix} S \\ B \end{bmatrix} = \begin{bmatrix} s & d \\ d & \mu \end{bmatrix} \begin{bmatrix} T \\ H \end{bmatrix} \quad (35)$$

where  $S$  is the strain,  $B$  is the magnetic flux density,  $s$  is the compliance,  $d$  is the strain coefficient,  $\mu$  is the permeability constant,  $T$  is the stress, and  $H$  is the magnetic field strength.

This set of equations is identical to a piezoelectric material except that  $D$  and  $E$  are replaced by  $B$  and  $H$ , respectively, and  $\varepsilon$  is replaced by  $\mu$ . Therefore, the derivation of the coupling coefficient and maximum output power are identical to the piezoelectric case, and only the results are given here.

$$k^2 = \frac{d^2}{s\mu} = \frac{d^2 Y}{\mu} \quad (36)$$

$$p_{\max} = \frac{k^2 \rho (QA)^2}{4\omega} \quad (26)$$

Note again, that the equation for power density is the same as for electromagnetic and piezoelectric transducers, and so has been numbered 26 as done previously.

While these equations do assume small signal behavior and ignore hysteresis, they do provide a good starting point for a broad comparison of technologies that could be used for inertial energy scavenging. It should be stated that, to the author's knowledge, no magnetostrictive energy scavengers have yet been designed.

### Electrostatic Application

The constitutive equations for electrostatic transducers depend heavily on the geometry and operating conditions (e.g., constant voltage or constant charge). Furthermore, they are usually not linear relationships. It is not possible to present the complete range of possibilities within this article. Rather, one common representative example will be covered.

Assume a parallel plate capacitive transducer as shown in Figure 5. The top plate of the capacitor oscillates between a minimum capacitance position (maximum gap between plates) and a maximum capacitance position (minimum gap). Assume that the capacitor is charged and discharged very rapidly compared to the period of mechanical oscillation. Therefore, the capacitive structure is operating under constant charge virtually all the time. See Meninger et al. (2001) and Roundy et al. (2002) for a further explanation of the operation of capacitive vibration-based generators.

Assuming constant charge operation and ignoring any parasitic capacitance, the coupled constitutive equations are:

$$F = \frac{q^2}{2a_e \varepsilon_0} - k_{sp} z \quad (37)$$

$$q = C(z)V \quad (38)$$

$$C(z) = \frac{a_e \varepsilon_0}{d - z} \quad (39)$$

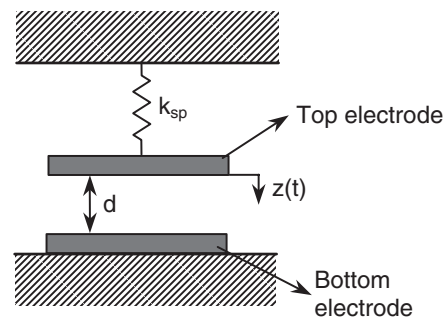


Figure 5. Standard parallel plate capacitive transducer.

where  $F$  is the force acting on the top plate,  $q$  is the charge on the top plate,  $V$  is the voltage across the capacitor,  $a_e$  is the electrode area,  $\epsilon_0$  is the permittivity constant, and  $C(z)$  is the capacitance of the structure.

In operation, the capacitive device is charged at some input voltage  $V_{in}$  in the maximum capacitance position ( $C_{max}$ ). The charge ( $q$ ), which is constant after the instantaneous charge is supplied from  $V_{in}$ , is given by

$$q = V_{in} C_{max} \quad (40)$$

As the structure is being used as an electrical generator, the stored energy at the output is the electrical energy stored in the capacitive device, and is given by

$$E_{elec} = \frac{q^2}{2C(z)} \quad (41)$$

The stored mechanical energy is given by

$$E_{mech} = \frac{1}{2} k_{sp} z^2 \quad (42)$$

The coupling coefficient is then given by

$$k^2 = \frac{E_{elec}}{E_{elec} + E_{mech}} = \frac{1}{1 + (E_{mech}/E_{elec})} \quad (43)$$

Substituting  $k_{sp} = m\omega^2$  into Equation (42), Equations (41) and (42) into (43), and simplifying yields the following expression for the coupling coefficient

$$k^2 = \frac{V_{in}^2 C_{max}^2}{V_{in}^2 C_{max}^2 + m\omega^2 z^2 C(z)} \quad (44)$$

Note that, as the electrostatic force is constant with respect to  $z$  in the constant charge case, there is no spring softening effect. However, the spring softening effect must be considered in the constant voltage case (see Yaralioglu et al., 2003).

As the capacitance ( $C(z)$ ) is a function of position, the coupling coefficient changes continuously throughout the operation of the generator. Although the expression derived here is valid only for parallel plate generators operating in a constant charge mode, it is usually the case that the coupling coefficient for electrostatic converters is dependent on position. The instantaneous maximum power transfer to the load can be calculated using Equation (26). The maximum energy density output per cycle can then be calculated as:

$$u_{out} = \frac{\rho(QA)^2}{4\omega^2} \int_{t_1}^{t_2} k(t)^2 dt \quad (45)$$

Finally, the output power density, averaged over time, for the load condition that maximizes the transfer coefficient is

$$p_{ave} = u_{out} f \quad (46)$$

where  $u_{out}$  is given by Equation (45) and  $f$  is the frequency in Hz ( $\omega/2\pi$ ).

## COMMON VIBRATION SOURCES

One of the aims of this study is to develop a simple means of calculating the maximum power that can be generated from a given vibration source. Thus, it is reasonable at this stage to review some characteristics of commonly occurring vibrations. The focus here is on relatively low-level vibrations that occur in common environments to make the discussion as broadly applicable as possible.

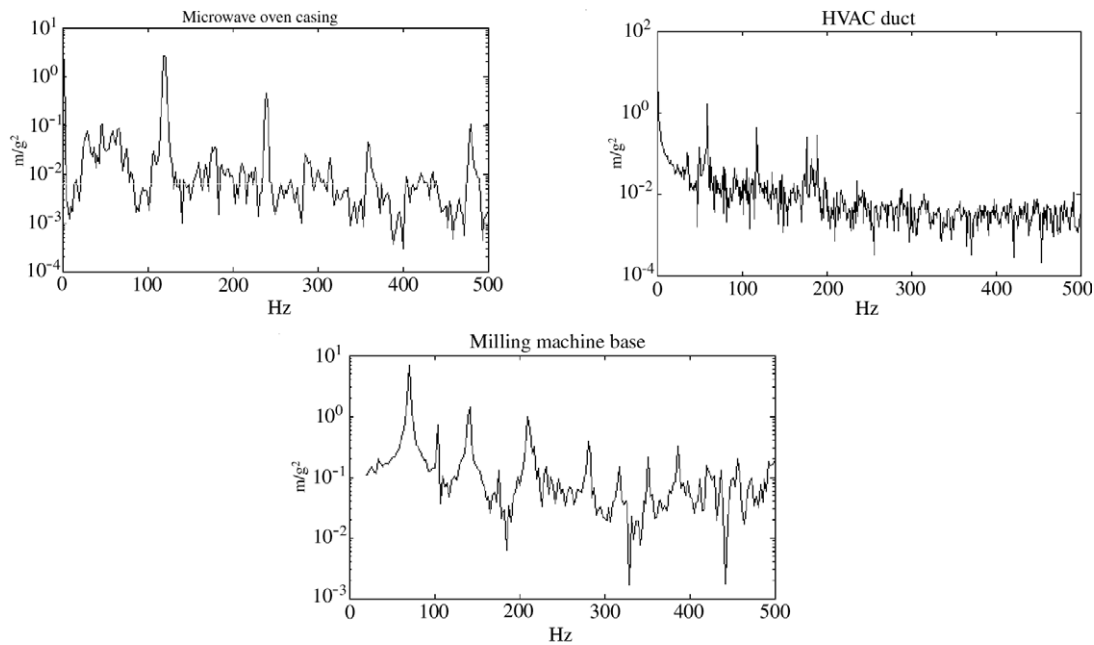
Data summarizing the results of measurements taken in from several vibration sources are shown in Table 1. The table lists the vibration source, the acceleration magnitude of the dominant vibration frequency, and the dominant (or peak) vibration frequency. Note that the dominant frequency is generally quite low, between 60 and 200 Hz for most cases. Note also that the acceleration magnitudes range from about 0.1 to 10 m/s<sup>2</sup> or 10 mg to 1 g. We will, therefore, focus on vibrations in this range.

Figure 6 shows the vibration spectra of a few of the sources listed in Table 1. Acceleration magnitude versus frequency is shown. The spectra shown in Figure 6 highlight two important points. First, as is the case with all sources listed in Table 1, the vibrations are concentrated at a single frequency and its harmonics. They are not broadband vibrations. Second, the acceleration magnitudes of the harmonics are significantly lower than those of the fundamental mode. As clearly shown by Equations (25) and (26), designs should target the vibration mode with the highest

**Table 1. Summary of several vibration sources.**

Vibration source	Peak acceleration (m/s <sup>2</sup> )	Frequency (Hz)
Base of 3-axis machine tool	10	70
Kitchen blender casing	6.4	121
Clothes dryer	3.5	121
Door frame just as door closes	3	125
Small microwave oven	2.25	121
HVAC vents in office building	0.2–1.5	60
Wooden deck with foot traffic	1.3	385
Breadmaker	1.03	121
External windows (2 ft × 3 ft) next to a busy street	0.7	100
Notebook computer while CD is being read	0.6	75
Washing machine	0.5	109
Second story floor of a wood frame office building	0.2	100
Refrigerator	0.1	240





**Figure 6.** Vibration spectra from the casing of a microwave oven, an HVAC duct in an office building, and the base of a milling machine.

acceleration magnitude, which is generally the lowest frequency mode.

## COMPARISON OF DIFFERENT TECHNOLOGIES

The preceding theory is meant to provide a simple basis both for comparing different approaches to vibration-based generation and for estimating the maximum possible power density that a given vibration source can theoretically supply. In the preceding discussion, the only parameter that distinguishes different technological (i.e., electromagnetic, piezoelectric, etc.) approaches is the coupling coefficient ( $k$ ). The quality factor ( $Q$ ) and density ( $\rho$ ) are design dependent, with physical limits of course. The acceleration magnitude ( $A$ ) and frequency ( $\omega$ ) of the input vibrations are outside the control of the designer. The purpose of this section is to compare different technologies, or in other words, to compare the coupling coefficients (and by extension the maximum transmission coefficient) of different technological approaches.

The coupling coefficient expressions in Equations (28) and (36) for piezoelectric and magnetostrictive materials are completely dependent on material properties. It should be noted that the overall coupling coefficient of a structure will differ from that of the underlying material. In the case of piezoelectric materials, the material coupling coefficient is dependent on the elastic and dielectric properties of the material. A structure containing piezoelectric material will likely have non-piezoelectric elastic elements and possibly dielectric elements. Therefore, the coupling of

**Table 2. Coupling and transmission coefficients for piezoelectric materials.**

Material	$k_{33}$	$k_{31}$	$\lambda_{33}$	$\lambda_{31}$
PZT-5A	0.72	0.32	0.175	0.027
PZT-5H	0.75	0.44	0.196	0.054
PVDF	0.16	0.11	0.006	0.003
PZN-PT	0.91	0.5	0.353	0.071

**Table 3. Coupling and transmission coefficients for magnetostrictive materials.**

Material	$k_{33}$	$\lambda_{33}$
Terfenol-D	0.6–0.85	0.11–0.28
Terzinol	0.95	0.411

the entire structure will differ from that of the piezoelectric material, which will probably make up a portion of the structure. Furthermore, supplementary loads to the structure may alter its elastic properties, which again will alter the overall coupling coefficient of the structure (see Lesieutre and Davis, 1997). While it may be possible that the coupling coefficient of a piezoelectric structure can exceed that of the material under certain circumstances, it is generally the case that the coupling coefficient of the material will exceed that of the structure. Table 2 shows the coupling and maximum transmission coefficients for some common piezoelectric materials, and Table 3 shows the coupling and maximum transmission coefficients for some magnetostrictive materials (Cullen et al., 1997).

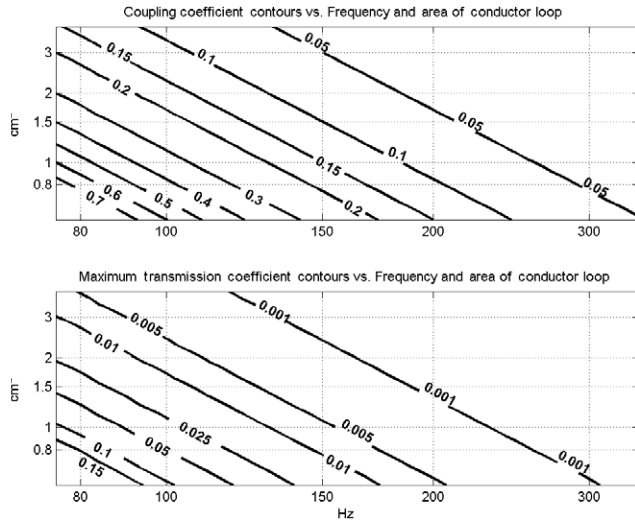


**Figure 7.** Coupling coefficient and maximum transmission coefficient contours for an electromagnetic converter vs frequency and area of the conductor (wire) loop. Density ( $\rho$ ) is  $7.5\text{ g/cm}^3$  and magnetic flux density ( $B$ ) is  $0.1\text{ T}$ .

The coupling coefficient equation for electromagnetic converters (Equation (17)) is dependent on design parameters. If we assume that the device consists of a cylindrical coil of radius  $r$  and length  $h$ , then we note the following relationships:  $l = 2N\pi r$  and  $L = \pi\mu_0 N^2 r^2 / h$  where  $N$  is the number of turns in the coil and  $\mu_0$  is the permeability of free space. We also note that  $k_{sp} = \rho v \omega^2$  where  $\rho$  is the density of the proof mass and  $v$  is the volume of the proof mass. We also assume that volume is roughly equal to  $\pi r^2 h$ . Substituting these relationships into Equation (17) yields the following expression for the coupling coefficient.

$$k^2 = \frac{4B^2}{\rho \omega^2 \mu_0 r^2} \quad (47)$$

Figure 7 shows the coupling coefficient contours and maximum transmission coefficient contours for electromagnetic generators versus frequency and the area enclosed by the conductor loop ( $\pi r^2$  in this case). The calculations were made assuming a density of  $7.5\text{ g/cm}^3$  and a magnetic flux density ( $B$ ) of  $0.1\text{ T}$ . Possible coupling coefficients for electromagnetic generators are comparable to those for piezoelectric and magnetostrictive technology converters.

As discussed in the previous section, the coupling coefficient for electrostatic devices is a function of position, and thus changes over time. Figure 8 shows the instantaneous coupling coefficient versus position of the top capacitor electrode relative to the bottom electrode. Notice that while the coupling coefficient has a maximum value of 1.0, the average value is far below 1.0.

An average coupling coefficient can be determined by simply calculating the average value of the coupling

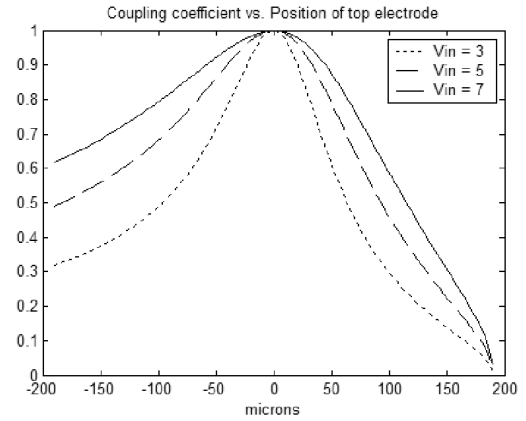


**Figure 8.** Coupling coefficient vs top electrode position for a parallel plate electrostatic generator for three different input voltages. Electrode area is  $1\text{ cm}^2$ , minimum capacitor gap is  $0.5\text{ }\mu\text{m}$ , density is  $7.5\text{ g/cm}^3$ , frequency is  $100\text{ Hz}$ , and  $Q$  is 30. Average power outputs corresponding to the three curves are  $3.8, 5.9,$  and  $7.5\text{ mW/cm}^3$ .

coefficient across the whole operating range. The coupling coefficient is very sensitive to the minimum allowable capacitor gap. Typically, this minimum gap is enforced with a mechanical stop. Figure 9 shows the average coupling coefficient for electrostatic generators versus operating frequency and minimum gap.

As with previous calculations, a quality factor ( $Q$ ) of 30 was used to generate the data in Figures 8 and 9. The nominal capacitor gap ( $d$ ) was determined as the magnitude of the oscillations that the top electrode would undergo at a  $Q$  of 30. So,  $d = Q \times A_{in} / \omega^2 + g_{min}$ , or  $195\text{ }\mu\text{m}$ , where  $g_{min}$  is the minimum allowable capacitor gap,  $0.5\text{ }\mu\text{m}$  in this case. Together with the data shown in Figures 8 and 9, these numbers highlight one of the issues with electrostatic generators. To design a generator with high power output, the range of motion of the generator must be hundreds of times greater than the minimum capacitor gap. This represents a practical implementation difficulty. If the nominal capacitor gap ( $d$ ) is designed to be much less than  $Q A_{in} / \omega^2$ , the effective quality factor ( $Q_{eff}$ ) will be much lower ( $Q_{eff} = d \omega^2 / A_{in}$ ). While the coupling coefficient would actually go up slightly in this case, the power output would go down (see Equations (44) and (46)). The first graph in Figure 10 shows the power output versus operating frequency and nominal capacitor gap for a minimum capacitor gap of  $0.5\text{ }\mu\text{m}$ . The second graph in Figure 10 shows the effective quality factor versus the same parameters. Note that for reasonable quality factors (10–50), the power output values are in the range of  $0.5\text{--}5\text{ mW/cm}^3$ . Furthermore, note that by decreasing  $d$ , both the power and effective quality factor decrease dramatically.

With the exception of electrostatic converters, the power expression given in Equation (26) applies to all technologies discussed. The only differentiator between technologies is the coupling coefficient. In fact, if the

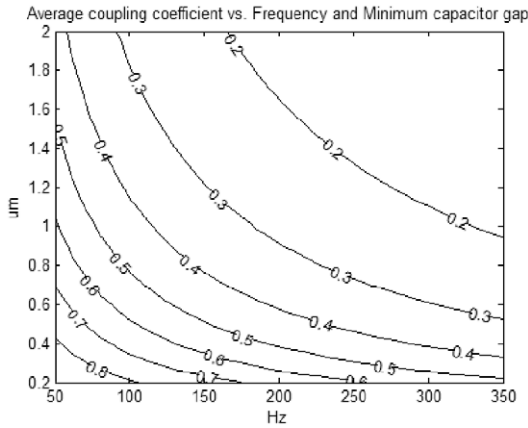


**Figure 9.** Average coupling coefficient contours vs frequency and minimum allowable capacitor gap for an electrostatic generator. Electrode area is  $1\text{ cm}^2$ , overall density is  $7.5\text{ g/cm}^3$ , and  $Q$  is 30.

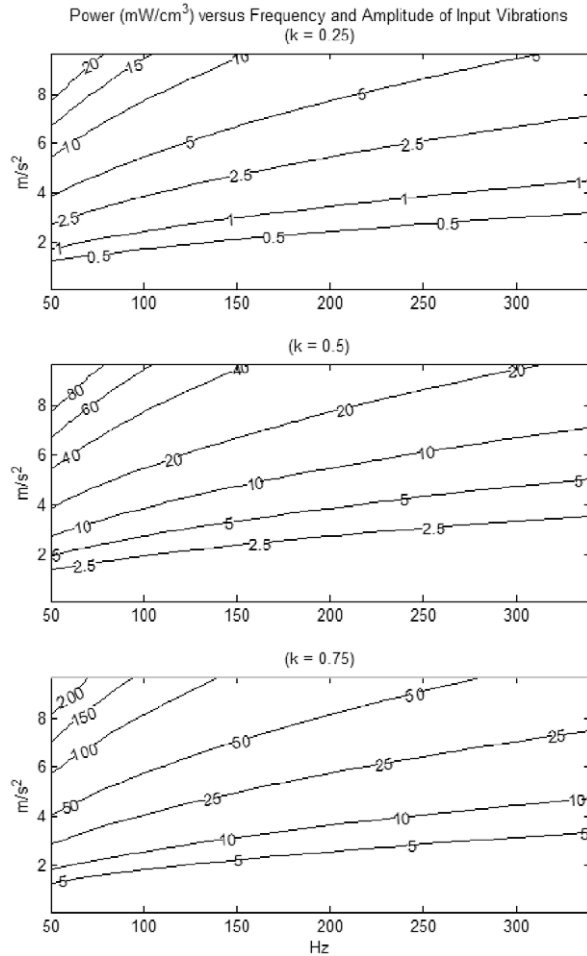


**Figure 11.** Power density ( $\text{mW/cm}^3$ ) contours vs frequency and acceleration amplitude of the input vibrations for three different coupling coefficients. Density ( $\rho$ ) is  $7.5\text{ g/cm}^3$  and quality factor ( $Q$ ) is 30.

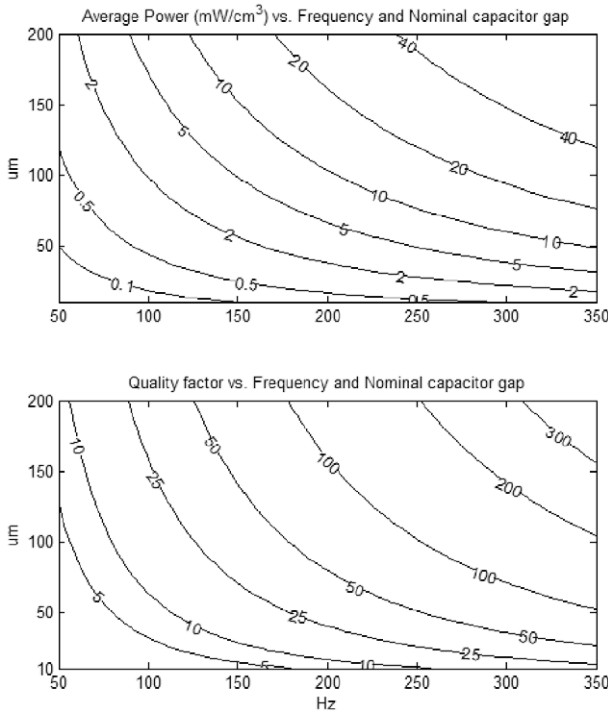


**Figure 10.** Average power output density contours ( $\text{mW/cm}^3$ ) and the necessary quality factor to obtain that power density vs operating frequency and nominal capacitor gap. The minimum capacitor gap is  $0.5\text{ }\mu\text{m}$ .

average coupling coefficient for electrostatic converters is used with Equation (26), the power estimates match those obtained with the technology-specific equations (44)–(46). Therefore, given the acceleration amplitude and frequency ranges of commonly occurring vibrations as shown in Table 1, and the coupling coefficients already presented, maximum power output values can be computed using Equation (26). Figure 11 shows the maximum power contours for a realistic input vibration range for three different coupling coefficients.

A density ( $\rho$ ) of  $7.5\text{ g/cm}^3$  was used for all calculations. This is roughly the density of steel. Note that the density figure in Equation (26) can be interpreted in two ways. First, it could represent the density of the proof mass. In this case, the power density number reflects on only the proof mass, not on the rest of the structure. Second, and perhaps more useful, the density could represent the proof mass divided by the entire converter volume. In this case, the power density takes into account the entire converter structure, and the designer can increase the density by minimizing empty space within the converter volume. In either case, power scales directly with density, and so the data shown in Figure 11 can easily be adjusted for different overall densities. A quality factor of 30 was assumed for these calculations.

While potential power density and efficiency are the primary subjects of this study, output voltage and current levels are also important in practical application, and can be a key differentiator between technologies.

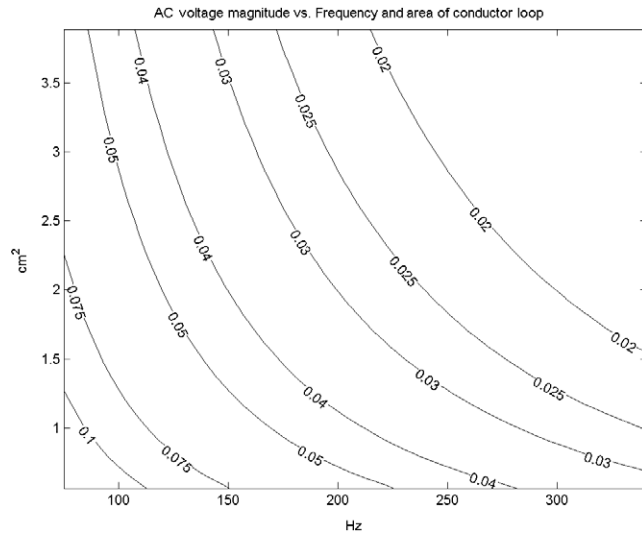


**Figure 12.** AC voltage magnitude contours for an electromagnetic converter vs frequency and area of the conductor loop. Acceleration of input vibrations is  $2.5 \text{ m/s}^2$  and number of turns per centimeter is 200.

Voltage contours versus frequency and area of the conductor loop for electromagnetic converters are shown in Figure 12. As demonstrated by the contours in Figure 12, low voltage output is frequently a problem for small electromagnetic converters.

As with all graphs in this section, Figure 12 is normalized per cubic centimeter. Therefore, as the area of the conductor loop increases, the length of the coil ( $h$ ) must decrease to maintain constant volume. As the length of the coil decreases, the number of turns also decreases. Since  $V = B/N\dot{z}$  where  $l$  is the length of one loop and  $N$  is the number of loops, the decrease in  $N$  translates to a decrease in the voltage. It is true that as area ( $a_1$ ) increases,  $l$  will also increase, but as  $l$  is proportional to  $\sqrt{a_1}$ , and  $N$  is proportional to  $1/a_1$ , the net effect of increasing the area of the conductor loop is to decrease voltage. In Figure 12,  $N$  was calculated using 200 turns per centimeter. If the volume were allowed to increase, keeping the coil length ( $h$ ) constant as area increased, the voltage would increase with increasing area.

Note that voltage decreases as frequency increases. This non-intuitive fact results from the assumption that the acceleration magnitude is fixed ( $2.5 \text{ m/s}^2$ ) across the whole frequency range, which is a reasonable assumption given the many vibration spectra measured as already reported. Thus, the velocity magnitude of the vibrations decreases as  $1/\omega$ , because of which the voltage also decreases as  $1/\omega$ .

In general, the voltage magnitude of electromagnetic converters increases with device volume. An increase in volume will increase the potential number of turns while keeping the area of each coil constant, thus increasing voltage. Piezoelectric devices suffer from the opposite

problem, usually exhibiting high voltages and low currents. The actual voltage and current outputs for a given power output depend on the type of converter structure used. Increasing the volume of piezoelectric material can either increase the voltage or the current produced depending on the way in which the volume of material is increased. However, as low voltage is rarely a problem for piezoelectric converters, we can say that increasing the volume will generally increase the current from the device.

The voltage output of electrostatic devices can be determined in a fairly arbitrary manner by specifying the initial charge up voltage (electrostatic converters need to be charged up initially). However, the current output of electrostatic devices depends on the capacitance. Therefore, larger devices, with larger capacitances provide higher currents. Thus, in general, electromagnetic converters can be scaled down in size at the cost of output voltage while piezoelectric and electrostatic converters can be scaled down only at the cost of current output.

## VIBRATION GENERATOR EFFECTIVENESS

It is often useful to have a figure of merit that can be used to compare dramatically different designs or approaches to vibration generator effectiveness. In many cases, efficiency is an appropriate figure of merit. If efficiency is defined synonymously with transmission coefficient, as seems natural, it is problematic for use as a figure of merit regarding vibration-based generators. First, the actual transmission coefficient (see Equation (7)) is dependent on the operating load condition. While the maximum transmission coefficient, as defined in Equation (13), is only dependent on the coupling coefficient, it does not take into consideration the quality factor ( $Q$ ) of the design, nor the overall density ( $\rho$ ) of the design, both of which play an important role in determining the output power density.

To address this problem, we will define a dimensionless figure of merit that we will call 'effectiveness'. First, given the theory presented already, consider how a designer could maximize power output for a given generator size. The first would be to design the generator with the maximum possible system coupling coefficient. The second would be to minimize the mechanical loss in the system, which is equivalent to maximizing the quality factor ( $Q$ ). A third consideration is the overall density ( $\rho$ ) of the design. By increasing the density of the proof mass, and decreasing the empty space within the generator, the overall density is improved. Finally, the designer should design the load to maximize power transfer,

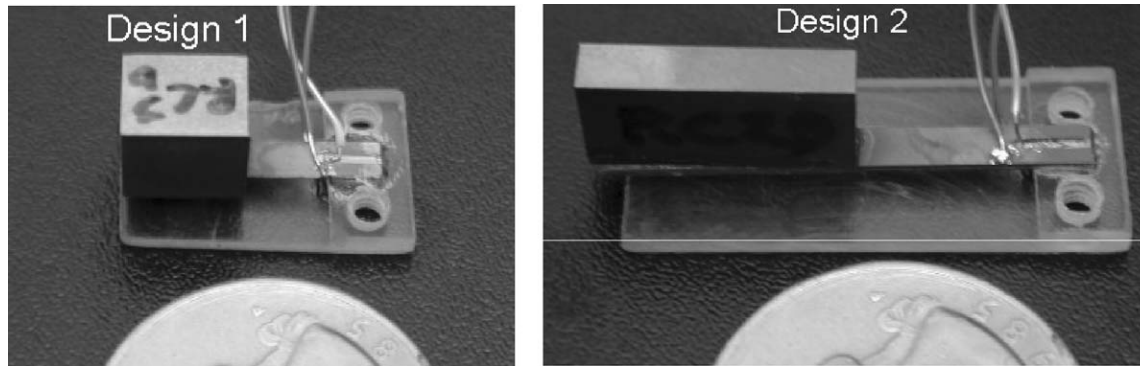


**Figure 13.** Two piezoelectric generators consisting of piezoelectric bimorphs mounted as cantilever beams.

which is the same as maximizing the transmission coefficient. Research on power circuit designs that maximize power output (Ottman et al., 2003) can be classified here as efforts to improve the actual (not maximum) transmission coefficient. In terms of the discussion here, it does not matter if such power circuits are linear or not as long as the transducer itself exhibits linear behavior. The improved power circuit will then improve the transmission coefficient ratio ( $\lambda/\lambda_{\max}$ ). Therefore, the following dimensionless term for ‘effectiveness’ is defined.

$$e = k^2 Q^2 \frac{\rho}{\rho_0} \frac{\lambda}{\lambda_{\max}} \quad (48)$$

where  $e$  is the effectiveness,  $\rho_0$  is a baseline density (perhaps  $7.5 \text{ g/cm}^3$  as used in this article),  $\rho$  is the actual density of the design,  $\lambda$  is the actual transmission coefficient, and  $\lambda_{\max}$  is the maximum transmission coefficient as defined in Equation (14).

The general power expression shown in Equation (26) was derived under the assumption that the generator was operating at its maximum transmission coefficient. Noting that power output is directly proportional to the transmission coefficient (see Equation (15)), the actual power density ( $p$ ) can be expressed as:

$$p = p_{\max} \frac{\lambda}{\lambda_{\max}} = \frac{k^2 \rho (QA)^2}{4\omega} \frac{\lambda}{\lambda_{\max}} \quad (49)$$

Substituting Equation (48) into Equation (49) yields the following expression for power output:

$$p = \frac{e \rho_0 A^2}{4} \frac{1}{\omega} \quad (50)$$

Thus, the power is dependent only on the design effectiveness, the baseline density, and the parameters of the input vibrations. Therefore, dramatically different designs can easily be compared by simply comparing their effectiveness assuming that the same baseline density is used in those calculations.

## COMPARISON TO EXPERIMENTAL RESULTS

In general, published experimental results for vibration-based generators indicate power levels significantly below the maximum power output that the simplified theory presented in this article would predict. First, it should be noted that often the coupling coefficient of the overall device is quite low and the overall density of the device is significantly lower than the  $7.5 \text{ g/cm}^3$  used herein. However, recall that the theory presented here assumes that the loading is such that the transmission coefficient, and thus power output, are at a maximum. It is generally not the case that generators are operating at this optimal level. The circuitry that loads the generator often is designed more to condition the power for use by an electronic device than to optimize the power transfer from the generator. Thus, the actual transmission coefficient is often well below the maximum transmission coefficient as given in Equation (14).

The concepts developed in this study are applied to the author’s experimental results using piezoelectric generators, some of which have been previously published (Roundy and Wright, 2004). The two generators consisting of piezoelectric bimorphs mounted as cantilever beams are shown in Figure 13.

The generators were driven at a vibration magnitude of  $2.25 \text{ m/s}^2$  at 85 Hz for Design 1 and 60 Hz for Design 2. Power was dissipated through a simple resistive load. The measured power output versus load resistance for the two generators is shown in Figure 14.

The coupling coefficient and quality factor were experimentally measured for each design. The coupling coefficient was determined by measuring the open circuit and short circuit natural frequencies and applying Equation (51) (Lesieutre, 1998). The damping ratio was measured by applying an impulse input to the system and measuring the resulting damped harmonic oscillation (James et al., 1994). Once the damping ratio is known, the quality factor is just  $Q = 1/(2\zeta)$ . The maximum transmission coefficient ( $\lambda_{\max}$ ) was then calculated from the measured coupling

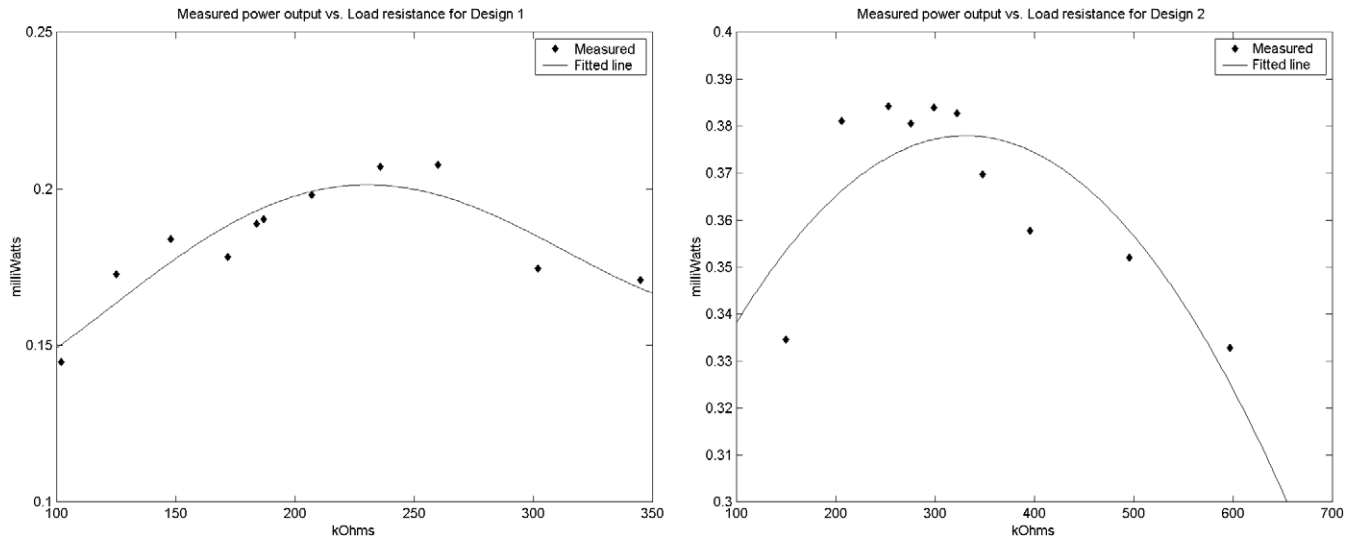


Figure 14. Measured power output vs load resistance for the two generators shown in Figure 13.

coefficient using Equation (14). The overall size (consisting of a rectangular cube placed around the beam and proof mass) of each design is 1 cm<sup>3</sup>. The  $k$ ,  $Q$ ,  $\rho$ , and  $\lambda_{\max}$  values for each design are shown in Table 4.

$$k_{\text{sys}}^2 = \frac{\omega_{\text{oc}}^2 - \omega_{\text{sc}}^2}{\omega_{\text{oc}}^2} \tag{51}$$

The relationship for power dissipated through a load resistor for the devices shown in Figure 13 has been previously published (Roundy and Wright, 2004). From Equation (49),  $\lambda/\lambda_{\max} = p/p_{\max}$ .  $p_{\max}$  can be obtained by using the optimal load resistance. Assuming a small value for  $k^2$ , as is the case for the designs presented here, the relationship between the transmission coefficient ratio ( $\lambda/\lambda_{\max}$ ) and the load resistance can be expressed analytically by the following equation:

$$\frac{\lambda}{\lambda_{\max}} = \frac{4R\omega C_p}{(1 + R\omega C_p)^2} \tag{52}$$

where  $C_p$  is the capacitance of the piezoelectric device.

Using Equation (52) and the data in Table 4, the theoretical effectiveness versus the load resistance for each design is shown in Figure 15.

Finally, the theoretical power versus load resistance can be calculated using Equation (50) and the effectiveness values in Figure 15. The theoretical and measured powers versus load resistance are shown in Figure 16 for each design.

Table 4. Parameter values for the two piezoelectric generators shown in Figure 13.

	$k$	$Q$	$\rho$ (g/cm <sup>3</sup> )	$\lambda_{\max}$
Design 1	0.12	17	7.45	0.004
Design 2	0.14	17	8.15	0.005

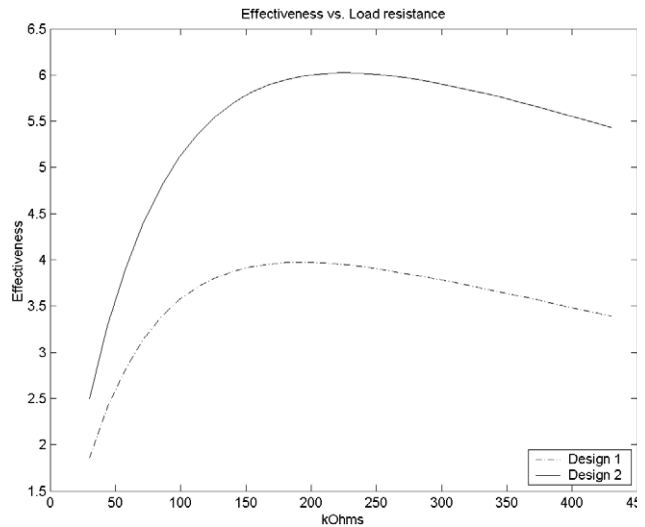


Figure 15. Theoretical effectiveness vs load resistance for each design shown in Figure 13.

Although the match between the theoretical and measured values is not perfect, the predictions are reasonably close and show the right trend. The theoretical predictions for Design 1 are about 30% too high, and predictions for Design 2 are about 10% too high. There are several possible reasons for the discrepancies. They may be due to unaccounted for losses. For example, first piezoelectric materials have an effective series resistance that was not modeled. Second, multiple measurements were taken for both the coupling coefficients and damping ratios. There was some variation in these measurements. A simple average value was used for theoretical predictions, which may also account for some of the error.

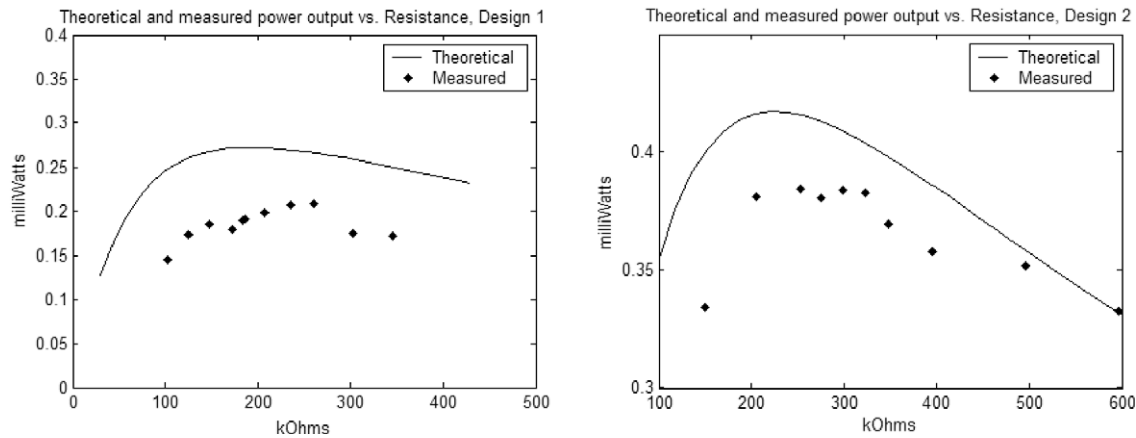


Figure 16. Theoretical and measured power output vs load resistance for the two designs in Figure 13.

## CONCLUSIONS

The purpose of this study is to provide a general theory upon which dramatically different types of vibration-based generators could be compared. The theory demonstrates that for any type of generator, the power output depends on the system coupling coefficient, the quality factor of the device, the density of the generator defined as the proof mass divided by the entire generator size, and the degree to which the electrical load maximizes power transmission (the transmission coefficient ratio). An expression for the 'effectiveness' of a vibration-based generator has been developed that incorporates all of these elements. The power output is, of course, also dependent on the magnitude and frequency of the input vibrations. Estimates of potential power output based on the theory presented have been given for a range of commonly occurring vibration sources. Estimates of maximum potential power density range from  $\approx 0.5$  to  $100 \text{ mW/cm}^3$  for the range of vibrations ranging from 1 to  $10 \text{ m/s}^2$  at frequencies from 50 to 350 Hz.

The general theory was applied to electromagnetic, piezoelectric, magnetostrictive, and electrostatic transducer technologies. The primary differentiator, in terms of power output, between different technologies is the coupling coefficient. Calculations show that, depending on material types and operation parameters, relatively high coupling coefficients (0.6–0.8) are possible for each of these technologies. The most suitable technology, therefore, needs to be decided upon based on the operating environment and the constraints of the design problem.

Some of the considerations are as follows. Electromagnetic generators tend to produce very low AC voltages. Furthermore, the voltage output scales down as the size scales down. Piezoelectric generators tend to produce high voltages and lower currents. For both piezoelectric and electrostatic generators, current, not voltage, will scale down with size because the

capacitance of device in general decreases with decreasing size. Finally, generating a level of power comparable to other technologies with electrostatic generators requires that the device oscillates at a magnitude of hundreds of microns while maintaining a minimum capacitive air gap of  $\approx 0.5 \mu\text{m}$  or less. This situation presents practical implementation and stability issues.

The concept of design 'effectiveness' was applied to two piezoelectric generators, and used to calculate theoretical power outputs. The power predicted by the effectiveness theory was about 30% more than the measured power output for one design and 10% more for the other design. Possible reasons for the discrepancies are unmodeled series resistance and variability in the measured coupling coefficients and damping ratios. Additional experiments need to be conducted to more carefully identify the discrepancy.

While the general theory presented contains many simplifications that may be unrealistic in certain cases, the author believes that the theory is useful primarily because of its generality. It provides a starting point from which to develop an overall theory of effectiveness for vibration-based generators, and a method for comparing dramatically different design concepts.

## REFERENCES

- Amirtharajah, R. and Chandrakasan, A.P. 1998. "Self-Powered Signal Processing Using Vibration-Based Power Generation," *IEEE Journal of Solid State Circuits*, 33(5):687–695.
- Bright, C. 2001. "Energy Coupling and Efficiency," *Sensors* (www.sensormag.com), 18(6).
- Ching, N.N.H., Wong, H.Y., Li, W.J., Leong, P.H.W. and Wen, Z. 2002. "A Laser-micromachined Multi-modal Resonating Power Transducer for Wireless Sensing Systems," *Sensors and Actuators A (Physical)*, 97–98:685–690.
- Cullen, J.R., Teter, J.P., Wun-Fogle, M., Restorff, J.B. and Clark, A.E. 1997. "Magnetic and Magnetoelastic Studies of Single Crystal Tb06Dy04Zn at Low Temperatures," *IEEE Transactions on Magnetics*, 33(5):3949–3951.
- El-hami, M., Glynne-Jones, P., White, N.M., Hill, M., Beeby, S., James, E., Brown, A.D. and Ross, J.N. 2001. "Design and

- Fabrication of a New Vibration-based Electromechanical Power Generator," *Sensors and Actuators A (Physical)*, 92:335–342.
- Glynn-Jones, P., Beeby, S.P., Jame, E.P. and White, N.M. 2001. "The Modelling of a Piezoelectric Vibration Powered Generator for Microsystems," In: *Transducers '01/Euroensors XV*, June 10–14, 2001, Munich, Germany.
- James, M.L., Smith, G.M., Wolford, J.C. and Whaley, P.W. 1994. *Vibration of Mechanical and Structural Systems*, Harper Collins College Publishers, New York, NY.
- Lesieutre, G.A. and Davis, C.L. 1997. "Can a Coupling Coefficient of a Piezoelectric Device Be Higher Than Those of Its Active Material?," *Journal of Intelligent Material Systems and Structures*, 8:859–867.
- Lesieutre, G.A. 1998. "Vibration Damping and Control using Shunted Piezoelectric Materials," *Shock and Vibration Digest*, 30:187–195.
- Meninger, S., Mur-Miranda, J.O., Amirtharajah, R., Chandrakasan, A.P. and Lang, J.H. 2001. "Vibration-to-Electric Energy Conversion," *IEEE Trans. VLSI Syst.*, 9:64–76.
- Mitcheson, P.D., Green, T.C., Yeatman, E.M. and Holmes, A.S. 2004. "Architectures for Vibration-Driven Micropower Generators," *Journal of Microelectromechanical Systems*, 13(3):429–440.
- Miyazaki, M., Tanaka, H., Ono, G., Nagano, T., Ohkubo, N., Kawahara, T. and Yano, K. 2003. "Electric-Energy Generation Using Variable-Capacitive Resonator for Power-Free LSI: Efficiency Analysis and Fundamental Experiment," In: *ISLPED 2003*, August 25–27, 2003, Seoul Korea.
- Ottman, G.K., Hofmann, H.F. and Lesieutre, G.A. 2003. "Optimized Piezoelectric Energy Harvesting Circuit Using Step-Down Converter in Discontinuous Conduction Mode," *IEEE Transactions on Power Electronics*, 18(2):696–703.
- Roundy, S., Wright, P.K. and Pister, K.S.J. 2002. "Micro-Electrostatic Vibration-to-Electricity Converters," In: *ASME IMECE*, Nov. 17–22, 2002, New Orleans, Louisiana.
- Roundy, S., Otis, B., Chee, Y.-H., Rabaey, J. and Wright, P.K. 2003b. "A 1.9 GHz Transmit Beacon using Environmentally Scavenged Energy," In: *ISLPED 2003*, August 25–27, 2003, Seoul Korea.
- Roundy, S. and Wright, P.K. 2004. "A Piezoelectric Vibration based Generator for Wireless Electronics," *Smart Materials and Structures*, 13:1131–1142.
- Sterken, T., Fiorini, P., Baert, K., Puers, R. and Borghs, G. 2003. "An Electret-Based Electrostatic m-Generator," In: *Transducers'03*, 2:1291–1294.
- Wang, Q.-M., Du, X.-H., Xu, B. and Cross, L.E. 1999. "Electromechanical Coupling and Output Efficiency of Piezoelectric Bending Actuators," *IEEE Transactions on Ultrasonics, Ferroelectrics, and Frequency Control*, 46(3):638–646.
- Yaralioglu, G.G., Ergun, A.S., Bayram, B. and Haeggstrom, E. 2003. "Calculation and Measurement of Electromechanical Coupling Coefficient of Capacitive Micromachined Ultrasonic Transducers," *IEEE Transactions on Ferroelectrics, and Frequency Control*, 50(4):449–455.